Biol Cybern (2011) 104:197–207
DOI 10.1007/s00422-011-0429-7

ORIGINAL PAPER

Biological Cybernetics

Block coherence: a method for measuring the interdependence between two blocks of neurobiological time series

Aatira G. Nedungadi · Mingzhou Ding · Govindan Rangarajan

Received: 13 July 2010 / Accepted: 19 February 2011 / Published online: 11 March 2011

Abstract Multisensor recordings are becoming commonplace. When studying functional connectivity between different brain areas using such recordings, one defines regions of interest, and each region of interest is often characterized by a set (block) of time series. Presently, for two such regions, the interdependence is typically computed by estimating the ordinary coherence for each pair of individual time series and then summing or averaging the results over all such pairs of channels (one from block 1 and other from block 2). The aim of this paper is to generalize the concept of coherence so that it can be computed for two blocks of non-overlapping time series. This quantity, called block coherence, is first shown mathematically to have properties similar to that of ordinary coherence, and then applied to analyze local field potential recordings from a monkey performing a visuomotor task. It is found that an increase in block coherence between the channels from V4 region and the channels from prefrontal region in beta band leads to a decrease in response time.

A. G. Nedungadi
Department of Mathematics, Indian Institute of Science, Bangalore 560012, India

Present Address:
A. G. Nedungadi
Computational Biology and Mathematical Modelling Group, Centre for Cellular and Molecular Biology, Hyderabad 500007, India

M. Ding
J. Crayton Pruitt Family Department of Biomedical Enginerring, University of Florida, Gainesville, FL 32611, USA

G. Rangarajan (✉)
Department of Mathematics and Centre for Neuroscience, Indian Institute of Science, Bangalore 560012 India
e-mail: rangaraj@math.iisc.ernet.in

Keywords Coherence · Spectral density matrix · Multivariate process · Granger causality

1 Introduction

In neuroscience, multielectrode technology is increasingly being used to simultaneously record neuronal activity in different regions of the brain to investigate the dynamics of large-scale functional networks (Bressler et al. 1993; Jain et al. 2001; Liang et al. 2002; Kus et al. 2004; Zhang et al. 2008). There exist many tools to investigate the resulting multivariate data (Kaminski and Blinowska 1991; Lutkepohl 1991; Bernasconi and Konig 1999; Friston et al. 2003; Harrison et al. 2003; Korzeniewska et al. 2003; Brown et al. 2004; Lungarella and Sporns 2006; Tang et al. 2008). Examples in the spectral domain include coherence and Granger causality (Granger 1969; Geweke 1982, 1984; Lutkepohl 1991; Boudjellaba et al. 1992; Rosenberg et al. 1998; Ding et al. 2000; Baccala and Sameshima 2001; Kaminski et al. 2001; Jarvis and Mitra 2001; Hesse et al. 2003; Brovelli et al. 2004; Chen et al. 2004; Roebroeck et al. 2005; Chen et al. 2006a,b; Ding et al. 2006; Dhamala et al. 2008a,b; Wu et al. 2008). There is, however, a lacuna in this suite of investigative tools. Currently, coherence is defined only between a pair of univariate processes (each modeling a single channel of observed data). Therefore, if one wants to assess the interrelationship between two regions of interest where each region is characterized by a set of more than one recording channels, coherence is not a convenient tool since it has to be computed individually for each pair and then somehow averaged over all pairs. Computing coherences for each pair does not take into account the internal dynamics within each region of interest. This can be properly accounted for only if

the data from all the channels in a given region are modeled as a realization of a multivariate stochastic process.

On the other hand, Granger causality does not suffer from the above shortcomings since it can be defined between two multivariate processes (Geweke 1982; Wang et al. 2007; Ladroue et al. 2009). Moreover, there exists a relation between Granger causality and coherence for a pair of univariate processes (Geweke 1982). By extending this relationship to a pair of multivariate processes, we propose a measure called *block coherence*. This quantity generalizes ordinary coherence to coherence between two multivariate processes which in turn can model time series data from two blocks of channels (or regions of interest). Block coherence is equivalent to generalized coherence defined by Pascual-Marqui (2007), a reference we were made aware of following the submission of the present work. However, in this paper, we rigorously study the properties of block coherence, introduce intra-block coherence, define partial block coherence, and point out situations where such measures can provide additional information.

If we consider all the channels, the number of pairwise coherences to be computed scales as $\binom{n}{2}$ where n is the number of channels (which is quite large in current imaging techniques). The number of block coherences to be computed scales only as $\binom{m}{2}$ where m is the number of regions of interest and m is typically much smaller than n. Even though computing ordinary coherences for a large ensemble of channels is feasible using nonparametric spectral methods, the computational cost becomes significant if one also wishes to assess the statistical significance of the computed ordinary coherences using random permutation tests via resampling.

It should be pointed out that measures like correlation and coherence only account for linear relationships. The brain is inherently a nonlinear system. Nevertheless, linear tools have been widely used in data analysis, as they are easy to compute and yield physiologically interpretable results. Further, nonlinear techniques require a much larger amount of data for analysis, which is not always experimentally feasible. In addition, one is often forced to analyze short time segments of data as the data from neuroscience experiments is typically non-stationary. This imposes a significant constraint on using nonlinear techniques to analyze neurobiological data.

The plan of the paper is as follows. In Sect. 2, we define block coherence and study its properties. We show that it has all the desirable properties that ordinary coherence has. Further, it reduces to ordinary coherence in the case of a pair of univariate processes. Numerical simulations are presented in Sect. 3 to illustrate the utility of block coherence. In Sect. 4, we apply block coherence to study the local field potential recordings from the brain of a monkey performing a visuomotor task. Conclusions and discussion are given in Sect. 5. Mathematical proofs of various results are given in the three appendices.

2 Block coherence

Let

$$X(t) = [X_1(t), X_2(t), \ldots, X_m(t)]^T,$$
$$Y(t) = [Y_1(t), Y_2(t), \ldots, Y_n(t)]^T,$$

denote an m-dimensional and an n-dimensional stationary stochastic processes, respectively (Lutkepohl 1991). Here T denotes the transpose. In this paper, we are interested in analyzing relationships between these two multivariate stochastic processes in the spectral domain.

2.1 Definition

We denote the $(m \times m)$-dimensional spectral density matrix of $X(t)$ by $S_{XX}(f)$

$$S_{XX}(f) = \begin{bmatrix} S_{X_1X_1}(f) & S_{X_1X_2}(f) & \cdots & S_{X_1X_m}(f) \\ S_{X_2X_1}(f) & S_{X_2X_2}(f) & \cdots & S_{X_2X_m}(f) \\ \vdots & \vdots & & \vdots \\ S_{X_mX_1}(f) & S_{X_mX_2}(f) & \cdots & S_{X_mX_m}(f) \end{bmatrix}, \quad (1)$$

where $S_{X_iX_j}(f)$ is the cross spectral density function (Percival and Walden 1998) of X_i and X_j at frequency f. Similarly, the $(n \times n)$-dimensional spectral density matrix of $Y(t)$ is denoted by $S_{YY}(f)$. Now consider the $(m+n)$-dimensional stochastic process

$$Z(t) = [X(t)^T, Y(t)^T]^T,$$

which we assume to be stationary. Denote the corresponding $(m+n) \times (m+n)$-dimensional spectral density matrix by $S_{ZZ}(f)$, or more explicitly as $S_{[X,Y]}(f)$.

We are interested in quantifying linear relationships between the two multivariate processes $X(t)$ and $Y(t)$ in the spectral domain. If $X(t)$ and $Y(t)$ are univariate processes, there already exists a widely used spectral domain measure called (ordinary) coherence (Lutkepohl 1991). The (ordinary) coherence between $X(t)$ and $Y(t)$ (for the univariate case) at frequency f is defined as

$$C_{XY}(f) \equiv \frac{|S_{XY}(f)|^2}{S_{XX}(f)S_{YY}(f)}. \quad (2)$$

If $X(t)$ and $Y(t)$ are multivariate, a measure of total linear association between $X(t)$ and $Y(t)$ can be defined as (Gel'fand and Yaglom 1959; Geweke 1982):

$$F_{X,Y} = \frac{1}{2\pi} \int_{-\pi}^{\pi} \ln \left(\frac{\det[S_{[X,Y]}(f)]}{\det[S_{XX}(f)] \det[S_{YY}(f)]} \right) \mathrm{d}f. \quad (3)$$

When $X(t)$ and $Y(t)$ are Gaussian, Eq. 3 is related to mutual information between $X(t)$ and $Y(t)$ (Gel'fand and Yaglom 1959; Brillinger and Guha 2007).

When $X(t)$ and $Y(t)$ are univariate, the above expression reduces to

$$F_{X,Y} = \frac{1}{2\pi}\int_{-\pi}^{\pi} \ln\left(1 - \frac{|S_{XY}(f)|^2}{S_{XX}(f)S_{YY}(f)}\right) \mathrm{d}f. \tag{4}$$

Further Eq. 4 can be shown to be equivalent to (Gel'fand and Yaglom 1959):

$$F_{X,Y} = \frac{1}{2\pi}\int_{-\pi}^{\pi} \ln\left(1 - C_{XY}(f)\right) \mathrm{d}f, \tag{5}$$

where $C_{XY}(f)$ is the ordinary coherence defined earlier.

We now propose a quantity that measures coherence between two multi-variate processes $X(t)$ and $Y(t)$. We call this quantity *block coherence* since each multidimensional stochastic process represents a block of channels in signal processing applications. We define block coherence such that it is related to $F_{X,Y}$ in the same way that ordinary coherence is related to $F_{X,Y}$ (for the case of univariate $X(t)$ and $Y(t)$). Thus, we have the following definition.

Definition Let $X(t)$ and $Y(t)$ be two multivariate stochastic processes, then the block coherence between $X(t)$ and $Y(t)$ at f is defined as

$$C_{XY}^{(B)}(f) \equiv 1 - \frac{\det[S_{[X,Y]}(f)]}{\det[S_{XX}(f)]\det[S_{YY}(f)]}, \tag{6}$$

where $S_{XX}(f)$, $S_{YY}(f)$, and $S_{[X,Y]}(f)$ are spectral density matrices of $X(t)$, $Y(t)$, and $\left[X^T(t), Y^T(t)\right]^T$, respectively.

Comparing with Eq. 3, we get

$$F_{X,Y} = \frac{1}{2\pi}\int_{-\pi}^{\pi} \ln\left(1 - C_{XY}^{(B)}(\lambda)\right) \mathrm{d}\lambda. \tag{7}$$

The above definition of block coherence was motivated by the univariate case. We now check that block coherence thus defined is well defined and has all the desired properties of coherence. The block coherence defined above is well defined for a given frequency f only if $S_{XX}(f)$ and $S_{YY}(f)$ are non-singular at that frequency. Note that the same situation exists even for ordinary coherence $C_{XY}(f)$ where $X(t)$ and $Y(t)$ are now univariate processes. $C_{XY}(f)$ is well defined at a frequency f only if S_{XX} and S_{YY} are non-zero at that frequency. Returning to block coherence, the spectral density matrices $S_{XX}(f)$ and $S_{YY}(f)$ can become singular at particular frequencies since these matrices are only guaranteed to be positive semi-definite (Rozanov 1967). If block coherence is to be well-defined for all frequencies, we need to impose the condition (as shown in Appendix A) that $X(t)$ and $Y(t)$ can be represented by finite order stationary autoregressive processes.

2.2 Properties of block coherence

Block coherence possesses properties similar to the properties of ordinary coherence.

Property 1

$$0 \le C_{XY}^{(B)}(f) \le 1, \ \forall f.$$

By using the generalized Hadamard's inequality (Friedland 1975; Mitrinovic et al. 1993), we can show that

$$\det[S_{[X,Y]}(f)] \le \det[S_{XX}(f)]\det[S_{YY}(f)]. \tag{8}$$

Using this inequality and the positive semi-definite property of spectral density matrices (Rozanov 1967), it is clear that $0 \le C_{XY}^{(B)}(f) \le 1 \ \forall \ f$.

Property 2 *If $X(t)$ and $Y(t)$ are uncorrelated at a frequency f then $C_{XY}^{(B)}(f) = 0$.*

Consider $X(t)$ and $Y(t)$ to be uncorrelated, then

$$S_{X_iY_j}(f) = 0, \quad i = 1, 2, \ldots, m; \quad j = 1, 2, \ldots, n.$$

Thus, $S_{[X,Y]}(f)$ is a block diagonal matrix (Horn and Johnson 1990) and hence $\det[S_{[X,Y]}(f)] = \det[S_{XX}(f)]\det[S_{YY}(f)]$. Hence from Eq. 6, $C_{XY}^{(B)}(f) = 0$ for all f.

Property 3 *If $X(t)$ and $Y(t)$ are completely correlated at a frequency f then $C_{XY}^{(B)}(f) = 1$.*

This follows from the fact $\det[S_{[X,Y]}(f)] = 0$ when $X(t)$ and $Y(t)$ are completely correlated at that frequency.

Property 4 *The block coherence reduces to ordinary coherence for univariate stochastic processes.*

This property can be easily deduced by calculating block coherence for a pair of univariate stochastic processes.

Property 5 *The block coherence reduces to multiple coherence when one block contains an univariate stochastic process.*

Let $X(t)$ be an univariate stochastic process and $Y(t)$ be an n dimensional stochastic process. Then the relevant spectral density matrices are

$$S_{XX}(f), \tag{9}$$

$$S_{XY}(f) = [S_{XY_1}(f) \cdots S_{XY_n}(f)], \tag{10}$$

$$S_{YX}(f) = S_{XY}^*(f), \tag{11}$$

$$S_{YY}(f) = \begin{bmatrix} S_{Y_1Y_1}(f) & S_{Y_1Y_2}(f) & \cdots & S_{Y_1Y_n}(f) \\ S_{Y_2Y_1}(f) & S_{Y_2Y_2}(f) & \cdots & S_{Y_2Y_n}(f) \\ \vdots & \vdots & & \vdots \\ S_{Y_nY_1}(f) & S_{Y_nY_2}(f) & \cdots & S_{Y_nY_n}(f) \end{bmatrix}. \tag{12}$$

Here $*$ denotes the Hermitian conjugate. The multiple coherence between $X(t)$ and $Y(t)$ is defined as

$$\gamma^2_{XY}(f) = \frac{S_{XY}(f)S^{-1}_{YY}(f)S_{YX}(f)}{S_{XX}(f)}. \tag{13}$$

Now, the block coherence between $X(t)$ and $Y(t)$ is given by (from (6))

$$\begin{aligned} C^{(B)}_{XY}(f) &= 1 - \frac{\det[S_{[X,Y]}(f)])}{\det[S_{XX}(f)]\det[S_{YY}(f)]} \\ &= 1 - \frac{(\det[S_{YY}(f)])}{\det[S_{XX}(f)]\det[S_{YY}(f)]} \\ &\quad \times \left(\det[S_{XX}(f) - S_{XY}(f)S^{-1}_{YY}(f)S_{YX}(f)]\right) \\ &= 1 - \frac{(\det[S_{YY}(f)])}{S_{XX}(f)\det[S_{YY}(f)]} \\ &\quad \times \left(S_{XX}(f) - S_{XY}(f)S^{-1}_{YY}(f)S_{YX}(f)\right) \\ &= \frac{S_{XY}(f)S^{-1}_{YY}(f)S_{YX}(f)}{S_{XX}(f)} \\ &= \gamma^2_{XY}(f). \end{aligned} \tag{14}$$

Here, we have used the properties of positive definite and partitioned matrices (Horn and Johnson 1990), the fact that $S_{XX}(f)$ and $S_{XY}(f)S^{-1}_{YY}(f)S_{YX}(f)$ are scalars (implying that $\det[S_{XX}(f) - S_{XY}(f)S^{-1}_{YY}(f)S_{YX}(f)] = S_{XX}(f) - S_{XY}(f)S^{-1}_{YY}(f)S_{YX}(f)$) and Eq. 13. Thus, block coherence reduces to multiple coherence in the above case.

Property 6 *If $S_{[X,Y]}(f)$ is positive definite at frequency f, its determinant decreases monotonically as the magnitudes of the cross spectral densities increases (see Appendix B for a proof) which in turn implies that the block coherence increases as the pairwise coherences increase.*

In summary, $C^{(B)}_{XY}(f)$ has all the properties of coherence and is clearly a proper generalization of ordinary coherence which is defined only for a pair of univariate stochastic processes.

For evaluation of the statistical significance of block coherence, one can use the random permutation test (Efron and Tibshirani 1993; Brovelli et al. 2004) when data from multiple trials is available. This random permutation procedure can be used to build a baseline null-hypothesis distribution from which statistical significance is derived. Consider two multivariate processes with many repeated realizations. We can reasonably assume that the data from different realizations are approximately independent of one another. Randomly pairing data for the first multivariate process with data for the second multivariate process from a different trial leads to the creation of a synthetic ensemble of trials for which there is no interdependence between the two processes based on construction, but the temporal structure within each process is preserved. Performing such random pairing with many different permutations will result in a distribution of block coherence corresponding to the null hypothesis of no statistical interdependence. The calculated value from the actual data is compared with this baseline null hypothesis distribution for the assessment of significance levels. A phase shuffling approach can also be used to generate null hypothesis distributions (Prichard and Theiler 1994).

2.3 Intra-block coherence

Definition Consider a single multivariate stochastic process $X(t)$. Its intra-block coherence is defined as

$$C^{(B)}_{XX}(f) \equiv 1 - \frac{\det[S_{XX}(f)]}{S_{X_1X_1}(f)S_{X_2X_2}(f)\ldots S_{X_mX_m}(f)}. \tag{15}$$

To be more precise, $C^{(B)}_{XY}(f)$ defined earlier [cf. Eq. 6] should be called the *inter-block coherence* and $C^{(B)}_{XX}(f)$ defined above the *intra-block coherence*.

Further, $C^{(B)}_{XX}(f)$ can be taken as the strength of the common reference signal present in all channels within the block. This would be particularly true if $X(t)$ is taken such that it comprises channels that are not expected to have any neurobiological interaction at that frequency.

Properties of Intra-block coherence

[i] Intra-block coherence takes values between 0 and 1.
[ii] One can easily show that as cross spectrum between the channels increases, the intra block coherence also increases (using the Theorem 2 in Appendix B).

2.4 Partial block coherence

Usually, systems are governed by more than two processes. These processes are directly or indirectly linked to each other. Partial coherence is a measure of coherence between a pair of univariate processes conditioned on another process (Albo et al. 2004; Schelter et al. 2008). Let $X(t)$, $Y(t)$, and $Z(t)$ be three univariate stochastic processes, then the partial coherence between $X(t)$ and $Y(t)$ conditioned on $Z(t)$ at f is defined in terms of partial spectral densities as

$$C_{XY|Z}(f) = \frac{\left[S_{XY|Z}(f)\right]}{\left[S_{XX|Z}(f)\right]\left[S_{YY|Z}(f)\right]}, \tag{16}$$

where partial cross spectral density conditioned on $Z(t)$ is given by

$$S_{XY|Z}(f) = S_{XY}(f) - \frac{S_{YZ}(f)S_{ZX}(f)}{S_{ZZ}(f)}. \tag{17}$$

This concept can be extended to multivariate processes. If $X(t)$, $Y(t)$, and $Z(t)$ are three multivariate stochastic processes, then the partial block coherence between $X(t)$ and $Y(t)$ conditioned on $Z(t)$ at f is defined as

$$C^{(B)}_{XY|Z}(f) \equiv 1 - \frac{\det[S_{[X,Y]|Z}(f)]}{\det[S_{XX|Z}(f)]\det[S_{YY|Z}(f)]}. \quad (18)$$

where

$$S_{XY|Z}(f) = S_{XY}(f) - S_{YZ}(f)S^{-1}_{ZZ}(f)S_{ZX}(f). \quad (19)$$

It can be shown that partial block coherence reduces to partial coherence for univariate stochastic processes. (see Appendix C for a proof.)

3 Numerical examples

3.1 Model

We consider a three channel system defined as follows:

$$x(t) = ax(t-1) + by(t-1) + \xi(t),$$
$$y(t) = dy(t-1) + \eta(t),$$
$$z(t) = gz(t-1) + hy(t-1) + \epsilon(t),$$

where $\xi(t)$, $\eta(t)$, and $\epsilon(t)$ are independent white noise processes with zero mean and variances σ_1^2, σ_2^2, and σ_3^2 respectively. We take $X_1(t) = [x(t), z(t)]^T$ as one block and $X_2(t) = y(t)$ as another block. The multivariate stochastic process comprising these three coupled processes is stationary if $|a|$, $|d|$ and $|g| < 1$ (Lutkepohl 1991). It turns out that block coherence between $X_1(t)$ and $X_2(t)$ can be computed exactly in this case and is given by:

$$C^{(B)}_{X_1X_2}(f) = \frac{\sigma_2^4(\sigma_1^2h^2 + \sigma_3^2b^2)}{(1 + d^2 - 2d\cos(2\pi f))\sigma_1^2\sigma_2^2\sigma_3^2 + \sigma_2^4(\sigma_1^2h^2 + \sigma_3^2b^2)}.$$

3.2 Numerical results

We generated 1000 realizations (trials) of the above process with 5000 points in each trial and for parameter values given by $a = 0.5$, $b = 0.5$, $d = 0.5$, $g = 0.5$, $h = 0.5$, and σ_1^2, σ_2^2 and $\sigma_3^2 = 0.01$. Assuming no knowledge of the underlying system, we then fitted a multivariate AR (MVAR) model of order 1 using standard procedure (Ding et al. 2000). Using this fitted MVAR model, we evaluated the required spectral density matrices and subsequently computed block coherence numerically. In Fig. 1, we have plotted both analytical as well as numerical results and it is clear that there is good agreement between the two.

3.3 Block coherence versus coherence

Consider the following two examples.

Example 1 Here the system consists of three channels, with first two channels in block 1 and the last channel in block 2. The system is defined as

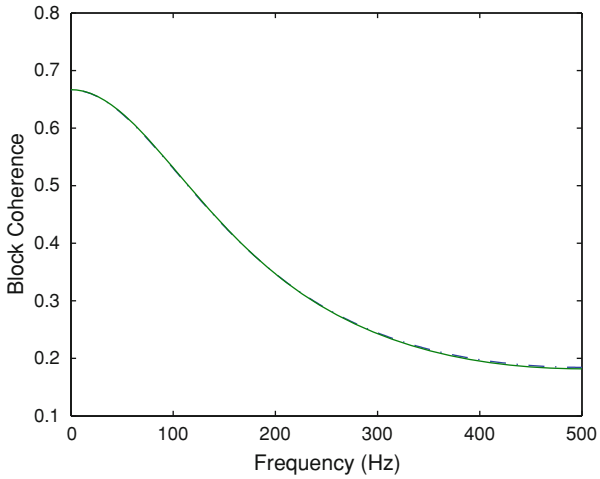

Fig. 1 Comparison of analytically (*solid line*) and numerically (*dashed line*) computed block coherence for the model system

$$x_1(t) = 0.1x_1(t-1) + 0.9y(t-1) + \epsilon_1(t), \quad (20)$$
$$x_2(t) = 0.1x_2(t-1) + 0.9y(t-1) + \epsilon_2(t), \quad (21)$$
$$y(t) = 0.1y(t-1) + \epsilon_3(t). \quad (22)$$

where the error covariance matrix for above system is given by

$$\Sigma_1 = \begin{bmatrix} 0.9 & 0.6 & 0 \\ 0.6 & 0.9 & 0 \\ 0 & 0 & 0.9 \end{bmatrix}. \quad (23)$$

Clearly, from the Eq. 23, we observe that the channels in block 1 are instantaneously interlinked.

Example 2 In this case the system is exactly defined as in Example 1 given by the Eq. 20–22. But the error covariance matrix is given by

$$\Sigma_2 = \begin{bmatrix} 0.9 & 0 & 0 \\ 0 & 0.9 & 0 \\ 0 & 0 & 0.9 \end{bmatrix}. \quad (24)$$

This implies the channels in block 1 are not instantaneously interlinked to each other.

We initially computed the intra block coherence of the first block for both the cases and this is plotted in Fig. 2. Clearly, from the figure we see that the intra block coherence is greater in the case of Example 1. Next, we compared the mean pairwise coherence (that is, ordinary coherence computed for each pair and then averaged over all possible pairs) with block coherence between blocks 1 and 2 for both the examples. From Fig. 3, we observe that mean pairwise coherence is the same in both the cases whereas block coherence is greater in the second case.

The above examples show that the block coherence between two blocks of channels decreases if the intra-block coherence of one of the constituent blocks increases. Thus,

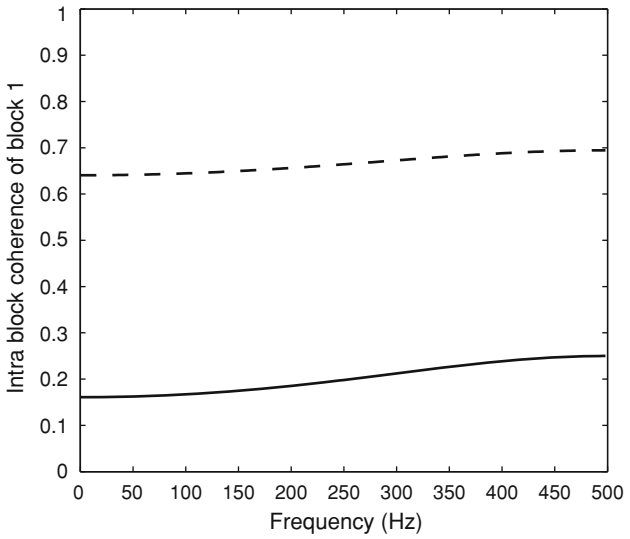

Fig. 2 Comparison of intra block coherence of the first block for both systems. Here *dashed line* represents intra block coherence of block 1 in Example 1 and *solid line* represents intra block coherence of block 1 in Example 2

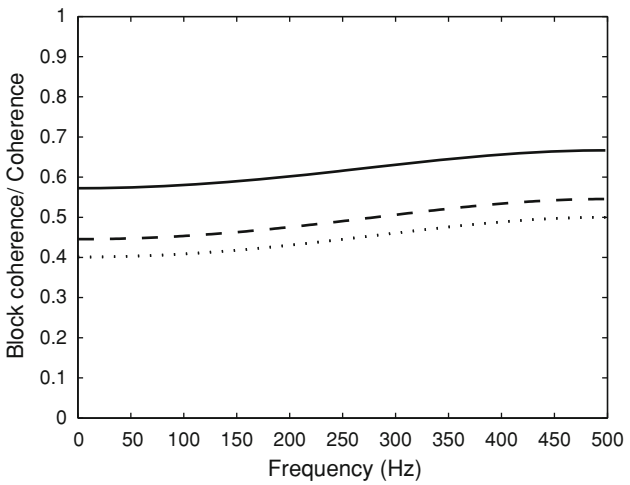

Fig. 3 Plot of mean pairwise coherence and block coherence for both the systems. Here *dashed line* represents block coherence in Example 1 and *solid line* represents block coherence in Example 2. *Dotted line* represents the coherence for both examples

block coherence can differentiate between Examples 1 and 2. But the mean pairwise coherence cannot distinguish between both examples without studying the noise covariance matrices. This is because block coherence (unlike pairwise coherence) models each block of channels as a realization of a multivariate stochastic process thus taking into account the internal relationships between the constituent channels within the block or region of interest. This is an advantage for block coherence over coherence specially in the case of nonparametric estimation where noise covariance matrices need not be estimated for the computation.

4 Experimental data

A monkey (TIO) was trained to perform a visuomotor task in the NIMH laboratory of Neuropsychology (Bressler et al. 1993) and the animal care was in accordance with institutional guidelines at that time. Surface to depth local field potentials were recorded from bipolar Teflon coated platinum electrodes chronically implanted in the left cerebral hemisphere. The monkey started each trial by depressing a lever with the right hand. Recording started 115 ms prior to the onset of the stimulus and continued till 500 ms post stimulus. Each stimulus consisted of four dots arranged in a slanted line or diamond pattern on a display screen. Monkey responded to the line pattern by releasing the lever (GO trial) and to the diamond pattern by continuing to hold the lever (NO-GO trial). Both patterns were presented with equal probability for all sessions. This stimulus–response contingency was switched in different recording sessions. We have analyzed the GO trials in this paper. The main interest is on how frontal-posterior network activity prior to stimulus onset facilitates visuomotor processing.

We focused our analysis on prestimulus data from five channels. Two channels (D and E) from V4 region formed block 1 and block 2 comprised three channels (L, M, and O) from prefrontal (PFC) region (see Fig. 4). The trials were sorted according to the ascending order of response time, and divided into 11 groups of 550 trials each, with 500 trials overlapping with the adjacent groups. A multivariate autoregressive model of order 15 was fitted to the data from each group using LWR algorithm (Morf et al. 1978). Once the fitted model parameters were available, the spectral density matrices could be easily computed (Ding et al. 2000). Substituting these in the expression for block coherence derived earlier, we obtained a parametric estimate of block coherence for each group.

In Fig. 5, mean block coherence spectrum, averaged over all 11 groups of trials, is plotted. Also using random permutation test with 1000 permutations, significance of these values (at $P = 0.01$ level of significance) was tested. The P-values here pertain to a particular frequency. Clearly this induces a multiple comparison problem over frequencies, which is confounded by the inherent correlations in block coherence. In principle, this can be overcome with random field theory (such as employed in Statistical Parametric Mapping). However, here, we simply refer to the uncorrected P-values. A significant peak around 20 Hz was clearly seen, indicating beta-band synchronized activity between PFC and V4.

Next we estimated the maximum block coherence value attained over the beta band (14–30 Hz) for each of the 11 groups. This peak block coherence was plotted against the mean response time for each group and shown in Fig. 6. The Spearman's rank correlation coefficient between the peak block coherence in the beta band and the mean response

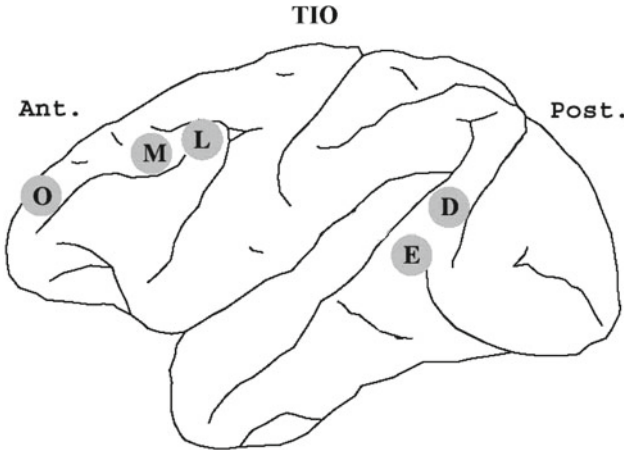

Fig. 4 Schematic diagram of electrode placement for monkey TIO. Data from V4 recording sites *D, E,* comprising block 1, and prefrontal recording sites marked *O, L*, and *M*, comprising block 2, are analyzed

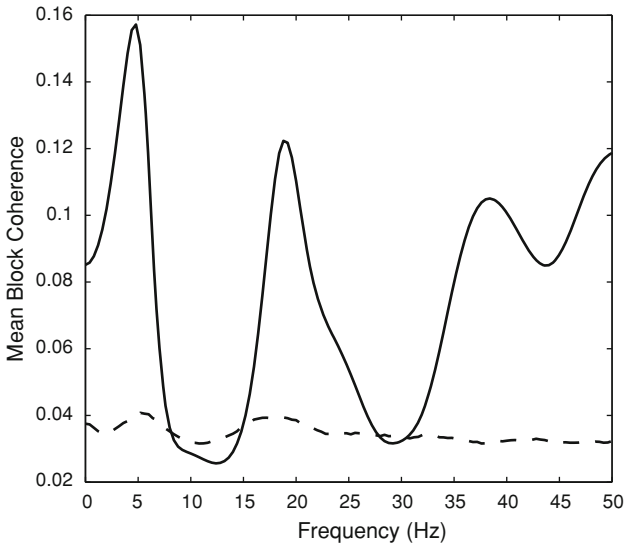

Fig. 5 Block coherence spectrum between V4 and prefrontal regions, averaged over different groups of trials sorted with respect to the response time. *Solid line* represents the actual value and the *dashed line* represents level of significance

time was found to be equal to -0.8000. This negative correlation, statistically significant at $P = 0.0114$, implies that a decrease in the block coherence between the channels from V4 region and the channels from prefrontal region in beta band leads to an increase in the response time. Recalling an earlier finding in PFC (Liang et al. 2002), where the negative correlation between the magnitude of prestimulus beta oscillation and RT led to the interpretation that PFC beta activity mediates anticipatory attention, the present result using block coherence can be seen as extending that finding to the PFC–V4 network.

The above analysis was repeated using mean pairwise coherence. Similar results were obtained. However, the computational effort involved in computing block coherence is smaller. In this particular case, given the small number of channels involved, the difference in computational effort is not dramatic. But in cases involving many channels per block, significant differences in computational effort would be observed.

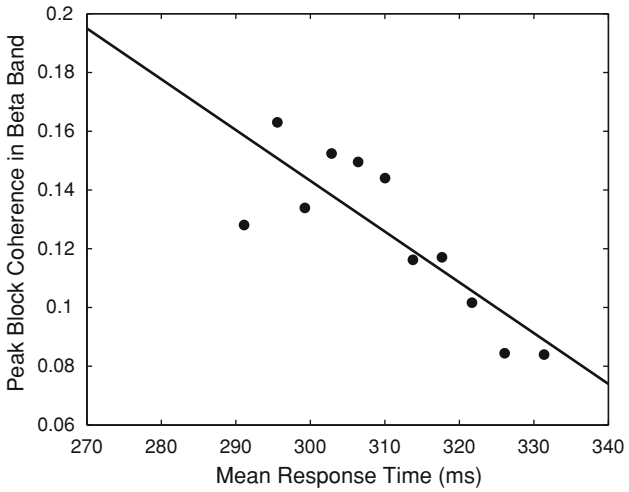

Fig. 6 A plot of peak block coherence (over the beta band) between V4 and prefrontal regions against the mean response time. The *straight line* corresponds to a least squares fit to the data

5 Conclusions

In this paper, we have studied a measure of coherence, called block coherence, between two multivariate stochastic processes. It is established that it is a valid generalization of the ordinary coherence to multivariate processes. Two related quantities, intra-block coherence and partial block coherence, are also defined and their properties studied. Block coherence can be used to find coherence between two regions of interest each containing a large number of channels. This measure offers one major advantage over ordinary pairwise coherence: It is better able to capture the internal dependencies between constituent channels within a region. When applied to experimental data, block coherence demonstrates that synchronized activity in beta band between prefrontal region and V4 facilitates visuomotor processing.

Acknowledgements AN was supported by a Fellowship from CSIR, India. MD was supported by NIH grant MH79388 and Air Force grant FA9550-07-1-0047. GR's work was supported in part by research grants from DRDO, DST Centre for Mathematical Biology (SR/S4/MS:419/07) and UGC-SAP (Phase IV). He is also associated with the Jawaharlal Nehru Centre for Advanced Scientific Research, Bangalore as an Honorary Faculty Member. We thank R. Coppola, R. Nakamura, and S.L. Bressler for providing us with the experimental data for the analysis.

Appendix A

We have seen in Sect. 2.1 that if the spectral density matrices $S_{XX}(f)$ and $S_{YY}(f)$ become singular at a particular frequency f, the block coherence $C_{XY}^{(B)}(f)$ is undefined at the frequency. In this Appendix, we show that $C_{XY}^{(B)}(f)$ is well defined for all frequencies if $X(t)$ and $Y(t)$ can be represented as finite order stationary multivariate autoregressive processes. Also we provide an example of infinite order autoregressive process where at some frequency f where the spectral density matrix become singular.

Lemma 1 *Let $X(t)$ be a finite order stationary m dimensional multivariate autoregressive process. Then the spectral density matrix $S_{XX}(f)$ is non-singular for all f.*

Proof Since $X(t)$ is assumed to be a multivariate autoregressive process, it can be represented as

$$X(t) = A(1)X(t-1) + A(2)X(t-2) + \cdots + A(p)X(t-p) + E(t), \tag{25}$$

where p is the order the autoregressive process, $A(i)$'s are $(m \times m)$ coefficient matrices, and $E(t)$ is the noise vector. Since the process is assumed to be stationary, the roots of the determinental equation

$$\det[I - A(1)z - A(2)z^2 - \cdots - A(p)z^p] = 0$$

lie outside the unit circle (Lutkepohl 1991). As the determinant is a polynomial in z, it can be written as

$$\det[I - A(1)z - A(2)z^2 - \cdots - A(p)z^p] = (z - z_1)(z - z_2)\cdots(z - z_p), \tag{26}$$

where $|z_i| > 1$ for all $i = 1, 2, \ldots, p$ are roots of the polynomial. Now rewriting Eq. 25 and then taking its Fourier transform, we get

$$[I - A(1)\mathrm{e}^{-i2\pi f} - A(2)\mathrm{e}^{-i4\pi f} - \cdots - A(p)\mathrm{e}^{-ip2\pi f}]X(f) = E(f).$$

We can write this as

$$G(f)X(f) = E(f), \tag{27}$$

where $G(f) = I - A(1)\mathrm{e}^{-i2\pi f} - \cdots - A(p)e^{-ip2\pi f}$.

Therefore, we have

$$\det[G(f)] = \det[I - A(1)z - \cdots - A(p)z^p],$$

where $z = \mathrm{e}^{-i2\pi f}$ which lies on the unit circle. This is nothing but the determinantal polynomial [cf. Eq. 26] encountered earlier. Since $X(t)$ is stationary, the roots z_i of the determinantal polynomial lie outside the unit circle. But $\det[G(f)]$ is obtained by evaluating this polynomial at z values lying on the unit circle. Hence $\det[G(f)] \neq 0, \forall f$. Thus, $G(f)$ is non-singular and so it can be inverted to obtain the following expression for $X(f)$:

$$X(f) = H(f)E(f), \tag{28}$$

where $H(f) = G^{-1}(f)$ and $\det[H(f)] \neq 0$. Now the spectral density matrix is given by

$$S_{XX}(f) = E[X(f)X^*(f)], \tag{29}$$

where $*$ denotes the Hermitian conjugate. This can be factorized as (Sayed and Kailath 2001),

$$S_{XX}(f) = H(f)\Sigma H^*(f), \tag{30}$$

where Σ is the covariance matrix of $E(t)$. But $\det[\Sigma] > 0$ since $X(t)$ is purely nondeterministic (Rozanov 1967). Hence

$$\det[S_{XX}(f)] = (\det[H(f)])^2 \det(\Sigma) > 0, \quad \forall f. \tag{31}$$

This proves that $S_{XX}(f)$ is non singular for all f. Similarly, if $Y(t)$ is also a stationary multivariate autoregressive process of finite order, $S_{YY}(f)$ is also non-singular. Consequently, from its definition in 6, $C_{XY}^{(B)}(f)$ is well-defined for all frequencies. □

We have shown above that the spectral density matrix is non-singular for all f if the autoregressive process is stationary and of finite order. Below we give an example of an infinite order autoregressive process where the spectral density matrix of the process is singular at a particular frequency.

Example Let $X(t)$ be a vector autoregressive process given by

$$\sum_{j=0}^{\infty} X(t-j) = E(t), \tag{32}$$

where $E(t)$ is noise vector with Σ as the covariance matrix. Now the backward shift operator B is defined as

$$B^j E(t) = E(t-j). \tag{33}$$

Using the backward shift operator, Eq. 32 can be written as $(I + B + B^2 + \cdots)X(t) = E(t)$ which can be simplified to

$$X(t) = (I - B)E(t). \tag{34}$$

Taking Fourier transform on both sides of Eq. 34 we get

$$X(f) = (I - I\mathrm{e}^{-i2\pi f})E(f). \tag{35}$$

Then by using Eqs. 29–30, we get

$$S_{XX}(f) = (I - I\mathrm{e}^{-i2\pi f})\Sigma(I - I\mathrm{e}^{-i2\pi f})^*, \tag{36}$$

where $*$ denotes Hermitian conjugate. Then

$$\det[S_{XX}(f)] = \left(\det\left[I - I\mathrm{e}^{-i2\pi f}\right]\right)^2 \det(\Sigma). \tag{37}$$

Clearly for $f = 0.5$, from Eq. 37, $S_{XX}(f)$ is singular.

This shows that block coherence (or for that matter, ordinary coherence) might not be well defined for all frequencies if no conditions are imposed. Even in such cases, block (or ordinary) coherence is defined for all frequencies except on a set of measure zero.

Appendix B

In this appendix, we show that Property 6 from Sect. 2.2 is true. We start with proofs of the following theorems.

Theorem 1 (Hadamard's inequality) *If* $A = ((a_{ij}))_{n\times n}$ *is positive semidefinite, then*

$$\det A \leq \prod_{i=1}^{n} a_{ii}. \tag{38}$$

Furthermore, when A is positive definite then equality holds if and only if A is diagonal.

Proof Refer to (Horn and Johnson 1990). □

Theorem 2 *The determinant of a positive definite hermitian* $n \times n$ *matrix considered as a polynomial in its off-diagonal terms, has only a single extremum. This extremum is attained when all the off-diagonal terms are zero and it is maximum.*

Proof Let $H = ((h_{ij}))_{n\times n}$ be a positive definite hermitian matrix. From the hermitean property,

$$h_{ij} = \overline{h_{ji}}, \forall i, j = 1, \ldots, n,$$

where $\overline{h_{ji}}$ denotes the complex conjugate of h_{ji}. Let us fix $i \neq j \in \{1, \cdots, n\}$. Without loss of generality we can assume $i < j$. Considering $\det H$ as a polynomial in the off-diagonal terms of H (while keeping the diagonal terms of H constant), we obtain the extrema of $\det H$ as follows:

$$\begin{aligned}
\frac{\partial \det H}{\partial h_{ij}} &= \frac{\partial}{\partial h_{ij}} \begin{vmatrix} h_{11} & h_{12} & \cdots & h_{1i} & \cdots & h_{1j} & \cdots & h_{1n} \\ \overline{h_{12}} & h_{22} & \cdots & h_{2i} & \cdots & h_{2j} & \cdots & h_{2n} \\ \vdots & \vdots & & \vdots & & \vdots & & \vdots \\ \overline{h_{1i}} & \overline{h_{2i}} & \cdots & h_{ii} & \cdots & h_{ij} & \cdots & h_{in} \\ \vdots & \vdots & & \vdots & & \vdots & & \vdots \\ \overline{h_{1j}} & \overline{h_{2j}} & \cdots & \overline{h_{ij}} & \cdots & h_{jj} & \cdots & h_{jn} \\ \vdots & \vdots & & \vdots & & \vdots & & \vdots \\ \overline{h_{1n}} & \overline{h_{2n}} & \cdots & \overline{h_{in}} & \cdots & \overline{h_{jn}} & \cdots & h_{nn} \end{vmatrix} \\
&= (-1)^{i+j} \begin{vmatrix} h_{11} & h_{12} & \cdots & h_{1j-1} & h_{1j+1} & \cdots & h_{1n} \\ \overline{h_{12}} & h_{22} & \cdots & h_{2j-1} & h_{2j+1} & \cdots & h_{2n} \\ \vdots & \vdots & & \vdots & \vdots & & \vdots \\ \overline{h_{1i-1}} & \overline{h_{2i-1}} & \cdots & h_{i-1j-1} & h_{i-1j+1} & \cdots & h_{i-1n} \\ \overline{h_{1i+1}} & \overline{h_{2i+1}} & \cdots & h_{i+1j-1} & h_{i+1j+1} & \cdots & h_{i+1n} \\ \vdots & \vdots & & \vdots & \vdots & & \vdots \\ \overline{h_{1n}} & \overline{h_{2n}} & \cdots & \overline{h_{j-1n}} & \overline{h_{j+1n}} & \cdots & h_{nn} \end{vmatrix} \\
&= H_{ij}.
\end{aligned} \tag{39}$$

where H_{ij} denotes the (i, j)th cofactor of H. □

In order to obtain the extremal points, the partial derivative of $\det H$ with respect to off diagonal terms of H is set equal to zero. Using the above equation, we get

$$\begin{aligned}
&\frac{\partial \det H}{\partial h_{ij}} = 0 \\
&\Rightarrow H_{ij} = 0, \ \forall i, j \in 1, \cdots n, i \neq j.
\end{aligned} \tag{40}$$

Since the diagonal terms of H are held constant, the above equation implies that there is only one extremum. Now, H is positive definite and hence its inverse exists (Hoffman and Kunze 1971) which is given by

$$H^{-1} = \frac{1}{\det H} \left((H_{ji})\right)_{n\times n}.$$

Evaluating the inverse at the extremal points of $\det H$ given by $H_{ij} = 0$ $(i \neq j)$, we get

$$H^{-1} = \frac{1}{\det H} \begin{bmatrix} H_{11} & \cdots & 0 \\ \vdots & & \vdots \\ 0 & \cdots & H_{nn} \end{bmatrix}.$$

Therefore, H^{-1} is a diagonal matrix and consequently H is a diagonal matrix at the point of extremum of $\det H$. To summarize, $\det H$ has only single extremum and it is attained at zero off diagonal terms of H. Clearly, at this extremum, determinant of H is product of its diagonal entries since H is a diagonal matrix at this extremum. Moreover, from Theorem 1, $\det H$ attains its maximum value at this extremum.

Property 6 *We are now in a position to show that Property 6 of block coherence listed in Sect. 2.2 is true. If the spectral density matrix* $S_{[X,Y]}(f)$ *at a frequency* f *is positive definite, then from the above theorem, the determinant of* $S_{[X,Y]}(f)$ *considered as a polynomial in the cross spectral densities, has only a single extremum at zero cross spectral densities and this extremum is a maximum. This implies that determinant of* $S_{[X,Y]}(f)$ *decreases as the cross-spectral densities increase. From the definition of block coherence [cf. Eq. (6)] we see that it increases if* $\det S_{[X,Y]}(f)$ *decreases. From the definition given in Eq. (2), we also see that (ordinary) pairwise coherence between* X_i *and* Y_j *increases if the magnitude of the cross-spectral density* $S_{X_iY_j}$ *increases. Putting everything together, we have proved that block coherence increases as the pairwise (ordinary) coherences increase.*

Appendix C

In this appendix, we show that partial block coherence reduces to partial coherence for univariate processes. The fact that it reduces to the traditional partial coherence indicates that block partial coherence can be interpreted the same way as the traditional partial coherence, namely, it measures the linear dependence between two blocks of time series at

a given frequency after the influences from other time series not in the two blocks have been statistically removed. Let $X(t)$, $Y(t)$ and $Z(t)$ be three univariate stochastic processes. Consider

$$S_{[X,Y]|Z}(f) = S_{[X,Y]}(f) - S_{[X,Y]Z}(f) S_{ZZ}(f)^{-1} S_{Z[X,Y]}(f). \tag{41}$$

Expanding Eq. 41, we get

$$S_{[X,Y]|Z}(f) = \begin{bmatrix} S_{XX}(f) & S_{XY}(f) \\ S_{YX}(f) & S_{YY}(f) \end{bmatrix} - \begin{bmatrix} S_{XZ}(f) \\ S_{YZ}(f) \end{bmatrix} S_{ZZ}^{-1} \begin{bmatrix} S_{ZX}(f) \\ S_{ZY}(f) \end{bmatrix}^T, \tag{42}$$

where T represent transpose. Simplifying and substituting from Eq. 19, we obtain

$$S_{[X,Y]|Z}(f) = \begin{bmatrix} S_{XX|Z}(f) & S_{XY|Z}(f) \\ S_{YX|Z}(f) & S_{YY|Z}(f) \end{bmatrix}. \tag{43}$$

Now substituting Eq. 43 in the definition of partial block coherence, we get

$$\begin{aligned} & C_{XY|Z}^{(B)}(f) \\ &= 1 - \frac{\det[S_{XX|Z}(f) - S_{XY|Z}(f) S_{YY|Z}^{-1}(f) S_{YX|Z}(f)]}{\det[S_{XX|Z}(f)]} \\ &= \frac{S_{XY|Z}(f) S_{YY|Z}^{-1}(f) S_{YX|Z}(f)}{S_{XX|Z}(f)} \\ &= \frac{S_{XY|Z}(f) S_{YX|Z}(f)}{S_{XX|Z}(f) S_{YY|Z}(f)} \\ &= \frac{\left|S_{XY|Z}(f)\right|^2}{S_{XX|Z}(f) S_{YY|Z}(f)} \\ &= C_{XY|Z}(f). \end{aligned}$$

This proves the result.

References

Albo Z, Viana Di Prisco G, Chen Y, Rangarajan G, Truccolo W, Feng J, Vertes RP, Ding M (2004) Is partial coherence a viable technique for identifying generators of neural oscillations. Biol Cybern 90:318–326

Baccala LA, Sameshima K (2001) Partial directed coherence: a new concept in neural structure determination. Biol Cybern 84:463–474

Bernasconi C, Konig P (1999) On the directionality of cortical interactions studied by structural analysis of electrophysiological recordings. Biol Cybern 81:199–210

Boudjellaba H, Dufour J, Roy R (1992) Testing causality between two vectors in multivariate autoregressive moving average models. J Am Stat Assoc 87:1082–1090

Bressler SL, Coppola R, Nakamura R (1993) Episodic multiregional cortical coherence at multiple frequencies during visual task performance. Nature 366:153–156

Brillinger D, Guha A (2007) Mutual information in the frequency domain. J Stat Plan Inference 137(3):1076–1084

Brovelli A, Ding, MZ, Ledberg A, Chen YH, Nakamura R, Bressler SL (2004) Beta oscillations in a large-scale sensorimotor cortical network: directional influences revealed by Granger causality. Proc Natl Acad Sci USA 101:9849–9854

Brown EN, Kass RE, Mitra PP (2004) Multiple neural spike train data analysis: state-of-the-art and future challenges. Nat Neurosci 7:456–461

Chen YH, Rangarajan G, Feng JF, Ding MZ (2004) Analyzing multiple nonlinear time series with extended Granger causality. Phys Lett A 324:26–35

Chen Y, Bressler SL, Knuth KH, Truccolo WA, Ding M (2006a) Stochastic modeling of neurobiological time series: power, coherence, Granger causality, and separation of evoked responses from ongoing activity. Chaos 16:026113

Chen Y, Bressler SL, Ding M (2006b) Frequency decomposition of conditional Granger causality and application to multivariate neural field potential data. J Neurosci Methods 150:228–237

Dhamala M, Rangarajan G, Ding M (2008a) Estimating Granger causality from Fourier and wavelet transforms of time series data. Phys Rev Lett 100(1–4):018701

Dhamala M, Rangarajan G, Ding M (2008b) Analyzing information flow in brain networks with nonparametric Granger causality. NeuroImage 41:354–362

Ding M, Bressler SL, Yang W, Liang H (2000) Short-window spectral analysis of cortical event-related potentials by adaptive multivariate autoregressive modeling: data preprocessing, model validation, and variability assessment. Biol Cybern 83:35–45

Ding M, Chen Y, Bressler SL (2006) Granger causality: basic theory and applications to neuroscience. In: Schelter B, Winterhalder M, Timmer J (eds) Handbook of time series analysis. Wiley-VCH Verlag, pp 437–460

Efron B, Tibshirani RJ (1993) An introduction to the bootstrap. Chapman and Hall/CRC, London

Friedland S (1975) Generalised Hadamard inequality and its application. Linear Multilinear Algebra 2:327–333

Friston KJ, Harrison L, Penny W (2003) Dynamic causal modeling. NeuroImage 19:1273–1302

Gel'fand IM, Yaglom AM (1959) Calculation of the amount of information about a random function contained in another such function. Am Math Soc Transl Series 2 12:199–246

Geweke J (1982) Measurement of linear dependence and feedback between multiple time series. J Am Stat Assoc 77:304–324

Geweke J (1984) Measures of conditional linear dependence and feedback between time series. J Am Stat Assoc 79:907–915

Granger C (1969) Measures of conditional linear dependence and feedback between time series. Econometrica 37:424–438

Harrison L, Penny WD, Friston KJ (2003) Multivariate autoregressive modeling of fMRI time series. NeuroImage 19:1477–1491

Hesse W, Moller E, Arnold M, Schack B (2003) The use of time-variant EEG Granger causality for inspecting directed interdependencies of neural assemblies. J Neurosci Methods 124:27–44

Hoffman KM, Kunze R (1971) Linear algebra. Prentice Hall, Englewood Cliffs, NJ, USA

Horn RA, Johnson CR (1990) Matrix analysis. Cambridge University Press, London

Jain N, Qi H-X, Kaas JH (2001) Longterm chronic multichannel recordings from sensorimotor cortex and thalamus of primates. Prog Brain Res 130:63–72

Jarvis MR, Mitra PP (2001) Sampling properties of the spectrum and coherency of sequences of action potentials. Neural Comput 13:717–749

Kaminski MJ, Blinowska KJ (1991) A new method of the description of the information flow in the brain structures by a modified directed transfer function (dDTF). Biol Cybern 65:203–210

Kaminski M, Ding M, Truccolo WA, Bressler SL (2001) Evaluating causal relations in neural systems: Granger causality, directed transfer function and statistical assessment of significance. Biol Cybern 85:145–157

Korzeniewska A, Manczak M, Kaminski M, Blinowska KJ, Kasicki S (2003) Determination of information flow direction among brain structures by a modified directed transfer function (dDTF)method. J Neurosci Methods 125:195–207

Kus R, Kaminski M, Blinowska KJ (2004) Determination of EEG activity propagation: pairwise versus multichannel estimate. IEEE Trans Bio-Med Eng 51:1501–1510

Ladroue C, Guo S, Kendrick K, Feng J (2009) Beyond element-wise interactions: identifying complex interactions in biological processes. PLoS ONE 4(9):e6899

Liang H, Bressler SL, Ding M, Truccolo WA, Nakamura R (2002) Synchronized activity in prefrontal cortex during anticipation of visuomotor processing. Neuroreport 13:2011–2015

Lungarella M, Sporns O (2006) Mapping information flow in sensorimotor networks. PLoS Comput Biol 2:1301–1312

Lutkepohl H (1991) Introduction to multiple timeseries analysis. Springer-Verlag, Berlin

Mitrinovic DS, Pecaric JE, Fink AM (1993) Classical and new inequalities in analysis. Kluwer Academic Publishers, Dordrecht

Morf M et al (1978) Recursive multichannel maximum entropy spectral estimation. IEEE Trans GeoSci Elec, GE-16 (2), 85–94

Pascual-Marqui RD (2007) Coherence and phase synchronisation: Generalisation to pairs of multivariate time-series and removal of zero led correlations. ArXiv:0706.1776v3

Percival DB, Walden AT (1998) Analysis for physical applications. Cambridge University Press, London, UK

Prichard D, Theiler J (1994) Generating surrogate data for time series with several simultaneously measured variables. Phys Rev Lett 73:951–954

Roebroeck A, Formisano E, Goebel R (2005) Mapping directed influence over the brain using Granger causality and fMRI. Neuroimage 25:230–242

Rosenberg JR, Halliday DM, Breeze P, Conway BA (1998) Identification of patterns of neuronal connectivity—partial spectra, partial coherence, and neuronal interactions. J Neurosci Methods 83:57–72

Rozanov YA (1967) Stationary random process. Holden Day, San Francisco

Sayed AH, Kailath T (2001) A survey of spectral factorization methods. Numer Linear Algebra Appl 8:467–496

Schelter B, Dahlhaus R, Leistritz L, Hesse W, Schack B, Kurths J, Timmer J, Witte H (2008) Multivariate time series analysis. In: Dahlhaus R, Kurths J, Maass P, Timmer J (eds) Mathematical methods in time series analysis and digital image processing. Springer, New York, pp 1–40

Tang A, Jackson D, Hobbs J, Chen W, Smith JL, Patel H, Prieto A, Petrusca D, Grivich MI, Sher A, Hottowy P, Dabrowski W, Litke AM, Beggs JM (2008) A maximum entropy model applied to spatial and temporal correlations from cortical networks in vitro. J Neurosci 28(2):505–518

Wang X, Chen Y, Bressler SL, Ding M (2007) Granger causality between multiple interdependent neurobiological time series: blockwise versus pairwise methods. Int J Neural Syst 17:71–78

Wu JH, Liu XG, Feng JF (2008) Detecting causality between different frequencies. J Neurosci Methods 167:367–375

Zhang Y, Chen Y, Bressler SL, Ding M (2008) Response preparation and inhibition: the role of cortical sensorimotor beta rhythm. Neuroscience 156:238–246